Journal of Engineering and Technology for Industrial Applications

ITEGAM-JETIA

Manaus, v.11 n.54, p. 7-24. July/August., 2025.
DOI: https://doi.org/10.5935/jetia. v11i54.1682

ISSN ONLINE: 2447-0228

RESEARCH ARTICLE OPEN ACCESS

PRODUCTION OF HYBRID BIODIESEL FROM A NOVEL TERNARY OIL BLEND: DUAL-STAGE PROCESS OPTIMIZATION USING DESIRABILITY BASED-RSM

Narcisse S. Nouadjep[1], César Kapseu[2] and Roland Solimando[3]

[1]Faculty of Engineering and Technology, University of Buea, P.O. Box 63, Buea, Cameroon.
[2]Department of Process Engineering, National School of Agro-Industrial Sciences,
University of Ngaoundere, P.O. Box. 455, Ngaoundere, Cameroon.
[3]Ecole Nationale Supérieure des Industries Chimiques (ENSIC) – Université de Lorraine, BP20451, Nancy Cedex, France

[1]http://orcid.org/0009-0003-0112-7839, [2]http://orcid.org/0009-0009-1424-654X, [3]http://orcid.org/0000-0003-0901-4196

Email: nouadjep@gmail.com, kapseu@yahoo.fr, roland.solimando@univ-lorraine.fr

ARTICLE INFO

Article History
Received: March 3, 2025
Revised: April 20, 2025
Accepted: June 15, 2025
Published: July 31, 2025

Keywords:
Esterification,
transesterification,
ANOVA,
neem,
shea butter.

ABSTRACT

The production of biodiesel is increasingly recognized as a sustainable alternative to fossil fuels. This study explores a two-step process for biodiesel production using a blend of Neem oil, Shea butter, and Waste kitchen oil. Process optimization was conducted using response surface methodology and the superposition approach, focusing on temperature, reaction time, ethanol-to-oil ratio, and catalyst concentration to maximize biodiesel yield. The model's performance was evaluated through R^2 and Absolute Average Deviation values. The highest desirability values obtained were 1 and 0.99 for the esterification and transesterification stages, respectively, with corresponding conversion yields of 94.57% and 90.53%. The analysis of the biodiesel revealed the presence of four distinct ethyl esters that are consistent with common fatty acid ethyl esters found in biodiesel. The hybrid biodiesel produced meets international standards, including ASTM and EN. Furthermore, the study achieved a high biodiesel yield with minimal catalyst usage (0.52 wt.%) and a short processing time (30 minutes), highlighting industries' potential to improve biodiesel production's economic viability by adopting similar optimized conditions.

I. INTRODUCTION

Energy is a critical requirement for human survival, and global energy consumption is expected to increase significantly in the 21st century. As demand for energy sources continues to grow, the need for efficient resource utilization becomes more pressing [1]. The scarcity of conventional energy sources, combined with rising global energy needs, highlights the importance of developing alternative fuels [2]. Although renewable and green energy technologies are gaining traction, they are yet to fully replace traditional fossil fuels [3]. Fossil fuels, such as coal, oil, and natural gas, have dominated the global energy landscape for decades, consistently accounting for over 80% of global energy production. This reliance has contributed significantly to environmental degradation due to carbon emissions [4],[5]. Despite advancements in technology and improvements in energy efficiency, the combined effects of population growth and economic expansion have driven up energy demand, outpacing the benefits of efficiency measures. The ongoing conflict between Russia and Ukraine has further exacerbated the energy crisis, causing substantial increases in household energy costs for heating, cooling, and transportation [6]. In 2021, over 45% of the European Union's gas supply was imported, representing nearly 40% of its total consumption [7]. The widespread use of non-renewable energy and rapid industrialization have significantly contributed to greenhouse gas emissions, environmental deterioration, and global temperature increases [8]. In 2021, global CO_2 emissions reached 36.6 gigatonnes, pushing projections for the rise in global surface temperature to approximately 3.5°C by 2100. The Paris Agreement of 2015 seeks to limit CO_2 emissions and keep the global temperature rise below 2°C compared to pre-industrial levels [9]. In response to the environmental and supply challenges posed by fossil fuels, researchers are intensifying efforts to identify clean and sustainable energy alternatives. These

efforts aim to reduce dependency on fossil fuels due to their finite nature, high greenhouse gas emissions, and harmful pollutants produced during combustion [10]. Under the Stated Policies Scenario (STEP) 2022 scenario, fossil fuel demand is expected to decline by 60% by 2050 [9]. By 2040, approximately 60 million tonnes of renewable fuels are projected to replace fossil fuels, reducing their use in the transportation sector to 85% [11]. The energy transition has increasingly shifted away from conventional bioenergy sources toward advanced biofuels [12] derived from sustainable feedstocks such as wasteland, marginal lands unsuitable for food crops, and waste streams [13],[14]. Biofuels, particularly biodiesel, have emerged as promising renewable energy sources due to their biodegradable, non-toxic nature and reduced emissions compared to conventional diesel [3],[15-17]. Biodiesel also exhibits superior chemical and physical properties compared to petroleum-based diesel [18]. Its use, whether in pure form or as a blend, has been shown to significantly lower emissions of combustion gases and carbon monoxide [19].

Biodiesel production can utilize various waste materials such as used cooking oils, animal fats, non-edible vegetable oils, and municipal waste as raw materials [20]. The concept of waste-based biodiesel originated during World War II and resurged during the 1970s energy crises when alternative fuel sources were sought due to shortages. By the 1980s, the transesterification method made it possible to produce biodiesel from waste materials [21]. This led to the classification of waste-based biodiesel as the second generation of biodiesel production [22]. Several methods are available for biodiesel production, including pyrolysis, dilution, microemulsion, and transesterification. Among these, transesterification has emerged as the most economically viable and practical approach, producing biodiesel with enhanced properties [23]. However, the efficiency and quality of biodiesel produced via transesterification are influenced by factors such as reaction time, temperature, catalyst concentration, feedstock type, and the methanol-to-oil ratio.

Optimizing these variables often requires extensive experimentation, which can be time-consuming, labor-intensive, and economically challenging [24]. To address this complexity, researchers have adopted empirical modeling techniques like Response Surface Methodology (RSM), which reduces the number of experimental runs while providing statistically robust results. For instance, [25] optimized biodiesel synthesis from refined cottonseed oil using a 2-level-4-factor RSM design, achieving a 96% yield. According to [26] applied RSM to optimize biodiesel production from animal fat, reporting a yield of 95.5%. For [27] used a Central Composite Rotatable Design (CCRD) to optimize a two-step biodiesel synthesis process from neem oil, achieving a maximum yield of 90.5%. Similarly, [28] optimized sunflower biodiesel production using CCRD, reporting a 95% yield.

Other studies have highlighted the impact of specific process parameters on biodiesel production. According to [29] optimized reaction variables such as molar ratio, catalyst concentration, and reaction time for waste cooking oil biodiesel, achieving a maximum yield of 94.15%. According to [30] optimized similar parameters for waste cooking palm oil biodiesel, reporting a yield of 79.7%. The Box-Behnken Design (BBD) has been found to be more efficient than CCRD and three-level full factorial designs [31]. BBD, when combined with RSM, enables effective estimation of second-order model coefficients, making it both economical and efficient for complex systems [32]. According to [33] utilized RSM-based BBD to optimize soybean biodiesel production, achieving a 94% yield. Charoenchaitrakool and Thienmethangkoon [34] applied the same approach to optimize a two-step catalyzed process for biodiesel production from waste frying oil, reporting a maximum yield of 90% and a free fatty acid (FFA) content as low as 0.5%. According to [24] achieved a 98.4% yield for Pongamia biodiesel using RSM-based BBD. Similarly, [35] optimized biodiesel production from esterified shea butter oil through transesterification using RSM with a BBD.

Sustainable biodiesel derived from various resources has emerged as a promising alternative to fossil fuels, with applications in marine propulsion, agriculture, small-scale power generation, and heavy freight vehicles [36]. According to [37] successfully developed a hybrid biodiesel using vegetable oil, butanol, and ethanol, all sourced from biomass. This hybrid biodiesel often demonstrates superior fuel properties compared to conventional biodiesel, with the optimal composition being 60% oil, 30% butanol, and 10% ethanol. Similarly, For [38] produced hybrid biodiesel from blended oils, achieving higher yields than fatty acid methyl esters (FAME) derived from single oil sources, with yields of 97.5%, 97.3%, and 97.9% for hazelnut, sunflower, and blended feedstocks, respectively.

According to [39] focused on biodiesel production and optimization using a combination of edible and non-edible oils, achieving a yield of 97.00% under specific reaction conditions. According to [40] explored biodiesel synthesis from a blend of radish oil and apricot kernel oil, highlighting the economic viability of this approach. For [41] investigated the production of biodiesel from a palm-sesame oil blend using ultrasound-assisted transesterification. In another study, According to [42] synthesized biodiesel from waste cooking oil and palm oil using a fly ash-derived catalyst, achieving a maximum yield of 73.8%. According to [43] produced biodiesel from a combination of pongamia and neem oils, while [44] optimized biodiesel production from a composite mixture of pongamia oil, animal fat oil, and waste cooking oil.

Their experiments, conducted at a molar ratio of 6:1 with 1.2 wt% catalyst, 64°C temperature, and 500 rpm agitation for 75 minutes, resulted in a maximum yield of 97.76%. According to [3] emphasized the sustainability of mixed oil feedstocks for biodiesel production, suggesting their potential for industrial-scale applications. According to [45] utilized RSM and Artificial Neural Networks (ANN) to optimize biodiesel yield from palm and cottonseed oil blends, achieving a yield of 96.32%. For [46] optimized biodiesel production from rice bran oil and sterculia foetida oil, reporting a methyl ester yield of 98.93% under ideal conditions. According to [47] applied RSM and ANN to optimize biodiesel production from a mixture of fish oil and rubber seed oil, achieving a yield of 91.5% by considering various independent input factors. For [48] study highlighted the favorable properties of biodiesel synthesized from a blend of four edible oils, meeting standard quality requirements.

After reviewing the literature, it has been observed that complex challenges like optimization can be effectively addressed through RSM. Numerous studies have successfully utilized this empirical mathematical tool to optimize biodiesel production parameters. However, most of these studies have focused solely on optimizing the alkali transesterification step, neglecting the acid esterification step required for high-FFA oils in a two-step biodiesel production process. Additionally, while individual oils have been extensively studied for biodiesel production, only a limited number of researchers have explored the use of mixed oils. The conversion of hybrid oils into biodiesel offers multiple advantages, including energy resource diversification, effective waste management, reduction of greenhouse gas emissions, economic stability, and climate change mitigation [49]. For instance, a recent study utilized mixed oils, combining three different vegetable oils to enhance the properties of the resulting biodiesel [50]. However, [51] applied the design of experiments,

specifically a basic lattice mixture design, to determine the optimal oil blending proportions (appropriate volume fractions) based on individual oil physicochemical characteristics. In their study significant emphasis was placed on developing a mixture model to establish the ideal oil blend ratios, thereby improving the properties of the mixed oil before proceeding with biodiesel production.

Furthermore, no research has been reported on optimizing the two-step biodiesel production process for a mixture of waste kitchen oil, Neem oil, and Shea butter using the BBD. This experimental work aims to address this gap by optimizing through desirability function in a two different single-objective optimization, the dual-stage biodiesel synthesis process using these high-FFA mixed oils. The study investigates the influence of key reaction parameters, including molar ratio, catalyst concentration, reaction temperature, and duration, on both the esterification and transesterification processes. The ultimate goal is to optimize the process for commercial implementation, reducing time and costs. Additionally, the paper presents the results of the characterization of the synthesized hybrid biodiesel, focusing on its shelf life and oxidative stability.

II. MATERIALS AND METHODS

II.1 MATERIALS

The hybrid vegetable oil (made of: neem oil, shea butter, and waste kitchen oil) used, was prepared according to [51]. For the transesterification reaction, ethanol with a purity of 98% from Sigma-Aldrich Reagent was utilized as the alcohol. Sulfuric acid (98% purity, Sigma-Aldrich Reagent) served as the acid catalyst, while potassium hydroxide (98% purity, Sigma-Aldrich Reagent) was used as the alkali catalyst.

II.2 METHODS

II.2.1. PRODUCTION OF BIODIESEL USING A TWO-STEP CATALYZED METHOD

The water content of the hybrid oil was determined to be 0.11% by weight and the FFA content of the hybrid oil utilized was determined to be 1.87%; which is notably high and could lead to soap formation if the reaction were conducted with an alkali catalyst, as indicated by [52]. Therefore, it was imperative to reduce the FFA content prior to the transesterification reaction with an alkali catalyst through a pretreatment step. Approximately 125 grams of the oil were heated to the desired temperature using a water bath and a magnetic hot plate stirrer equipped with a temperature controller (Stone Staffordshire, model HC-1202). The stirring speed was maintained at a constant 400 rpm throughout the experiment. Subsequently, predetermined quantities of sulfuric acid and ethanol were introduced into the oil. The oil-to-ethanol molar ratio is calculated based on the oil's molecular weight.

The heating and stirring were halted once the reaction had reached the preset reaction time. To stop the reaction, the flask was promptly immersed in cold water. Following the first step, the mixture was left to settle for 1 hour, resulting in the separation of two distinct liquid phases. The excess ethanol in the upper phase was removed using a separating funnel, while the lower phase contained ethyl ester and unreacted triglyceride was further subjected to a reaction with KOH in the second step (without removing the H2SO4 from the product of the first step). Upon completion of the second step reaction, the product obtained was left to settle overnight, resulting in the formation of two distinct liquid phases: an ester phase at the top and a glycerol phase at the bottom. The biodiesel product underwent multiple washes with deionized water until the washing became clear. Subsequently, the product was dried by heating at 100°C.

II.2.2. EXPERIMENTAL DESIGN

RSM-based BBD was employed using Design-Expert software to optimize FAEE yield in the biodiesel production process in two steps of transesterification. The optimization was carried out numerically within predefined ranges utilizing the desirability function, as outlined by [53]. This function involves the transformation of each predicted response into a dimensionless partial desirability function, which incorporates the researcher's priorities and preferences during the optimization process. Depending on whether each response needs to be maximized, minimized, or has a target value, one- or two-sided functions are employed. Essentially,

the desirability function consolidates all responses into a single metric, enabling the prediction of optimal levels for all independent variables, as explained by [54]. The desirability function was utilized to investigate how reaction temperature, ethanol-to-oil molar ratio, catalyst concentration, and reaction time affect biodiesel yield. The desirability function-based method involves transforming the estimated response models (typically second-order models) into individual desirability functions di(Yi). These individual functions are then combined into a composite function denoted as D. Typically, this composite function is either a geometric mean (optimized for maximization) or an arithmetic mean (optimized for minimization). The total desirability function established is represented in Equation (1). Here, wi represents a weight that is relative in importance among n responses.

$$D(Y) = \left(\prod_{i=1}^{n} d_i(y)^{w_i} \right)^{\frac{1}{\sum_{i=1}^{n} w_i}} \quad (1)$$

The weight controls how desirability is allocated within the interval between the lower (or upper) bound and the target value. It shapes the desirability function, which maps the response scale onto a normalized range from zero to one, facilitating the evaluation of individual response desirability. To maintain an accurate representation of process performance without introducing bias, each parameter's weight was assigned a value of one; resulting in a linear ramp function that transitions between the lower (or higher) and desired values.

Four distinct variables were considered: (A) temperature, (B) ethanol-to-oil molar ratio, (C) catalyst amount, and (D) time. The design was generated through Design-Expert® version 13 software (Stat-Ease Inc., Minneapolis, USA). Conducted in triplicate, Table 1 outlines the range and levels of the independent variables used in the experiments.

The data obtained from the two-stage experimental process were analyzed using the response surface regression method based on a second-order polynomial Equation (2).

$$Y = \beta_0 + \sum_{i=1}^{k} \beta_i X_i + \sum_{i=1}^{k} \beta_{ij} X_i^2 + \sum_{i1<j}^{k} \sum_{j}^{k} \beta_i X_i X_j + e \quad (2)$$

Here: Y denotes the predicted response, β_0 represents the intercept, β_i is the linear coefficient, β_{ii} is the quadratic coefficient, and β_{ij} is the interaction coefficient. The terms X_i and X_j refer to the independent variables.

Multiple regression was employed to link the response variable to the independent variables and to determine the coefficients of the polynomial response model. The model's fit quality was assessed through analysis of variance (ANOVA) and significance testing (with a significance level of $p < 0.05$). The process involved iterative correlation and the derivation of practical regression models. Concurrently, contour lines were generated based on empirical findings. The models' appropriateness was validated by assessing the Lack of Fit values and conducting the F-test, resulting in the selection of the most accurate results for each response variable.

Table 1: Range and levels of operating parameters of the hybrid oil dual stage conversion procedure.

Variables	Symbol coded	Range and levels		
		-1	0	1
1st Step: esterification				
Temperature (°C)	A	45	50	55
Ethanol to oil molar ratio	B	0.5:1	4.25:1	8:1
H_2SO_4 Concentration (wt.%)	C	0.50	1	1.50
Time (min)	D	30	45	60
2nd Step: transesterification				
Temperature (°C)	*A*	50	65	80
Ethanol to oil molar ratio	*B*	3.5:1	6.5:1	9.5:1
KOH Concentration (wt.%)	*C*	0.5	1.25	2
Time (min)	*D*	30	45	60

Source: Authors, (2025).

II.2.3. DETERMINATION OF ETHYL ESTER CONTENT AND DETERMINATION OF YIELD

The analysis of ethyl ester content in the product was carried out using Shimadzu's GCMS-QP 2010 Plus, equipped with the LabSolutions software, which offers a user-friendly interface for efficiently displaying sample chemical compositions. The LabSolutions GCMS software streamlines system operations by optimizing both data acquisition and analysis processes. It supports simultaneous acquisition and analysis of GC and MS data with ease and incorporates various features to enhance workflow efficiency. The chromatograph was equipped with a high-resolution RTxi-5ms capillary column. Compound identification was carried out using the integrated database from the American National Institute of Standards and Technology (NIST).

This analysis utilized Methyl Heptadecanoate (C17:0) as an internal standard and followed a method adapted from [55]. The percentage of ethyl ester was then calculated using Equation (3):

$$\%FAEE = \frac{(\sum A) - A_{EI}}{A_{EI}} x \frac{C_{EI}\, x\, V_{EI}}{W}\, x\, 100 \quad (3)$$

where:

- $\sum A$: This represents the total sum of all areas under the curve ranging from C14 to C24.
- A_{EI}: It signifies the area under the curve specifically for C17:0.
- C_{EI}: This denotes the concentration of C17:0 in milligrams per milliliter (mg/mL).
- V_{EI}: It represents the quantity of C17:0 utilized, measured in microliters (µL).
- W: Weight of the product (mg).

The product's yield was determined using the methodology outlined in [56] and [57], applying Equation (4).

$$\%Yield = \frac{weight\ of\ product(g)}{weight\ of\ raw\ oil(g)}\, x\, 100 \quad (4)$$

III. RESULTS AND DISCUSSIONS

III.1 DATA ANALYSIS AND MODELING

3.1.1. Esterification process

In the initial phase of the experiment, the esterification reaction was conducted to diminish the FFA content within the range of 45-55ºC using H_2SO_4 as the catalyst. Table 2 displays the BBD matrix concerning independent variables and the corresponding %FAEE values obtained. Notably, the %FAEE fluctuates between 73.14% and 92.85%. The highest percentage was achieved within the moderate temperature and acid concentration range, low ethanol molar ratio, and a longer reaction time. Conversely, the lowest %FAEE was observed at a high-temperature range, low acid concentration, and moderate levels of ethanol molar ratio and reaction time. The significance of each parameter was assessed using the p-value, and the results are documented in Table 3.

Table 2: BBD matrix with four variables for the esterification process.

Run	Temp. (°C)	Ethanol molar ratio	H_2SO_4 Conc. (wt,%)	Time (min)	%FAEE from expt.	%FAEE from Model
1	50	0,5	1,5	45	91,12	90,8
2	50	4,25	1	45	83,41	89,3
3	55	8	1	45	78,82	77,3
4	50	0,5	0,5	45	74,16	78,51
5	45	0,5	1	45	82,32	81,43
6	50	4,25	0,5	60	84,02	83,1
7	55	4,25	1,5	45	82,54	79,2
8	45	4,25	0,5	45	73,78	74,3
9	50	0,5	1	60	92,85	91
10	45	8	1	45	77,87	78,59
11	45	4,25	1	60	80,09	77,7
12	50	4,25	0,5	30	79,09	78,51
13	50	8	1	60	83,02	84,57
14	50	4,25	1,5	30	83,6	81,43
15	50	8	1	30	82,77	77,3
16	50	0,5	1	30	82,97	83,98
17	45	4,25	1	30	81,21	83,7
18	55	4,25	1	60	83,22	85,6
19	50	4,25	1	45	82,89	81,96
20	50	4,25	1	45	82,99	83,1
21	55	0,5	1	45	81,02	76,9
22	50	8	0,5	45	81,56	82,7
23	50	8	1,5	45	83,89	82,69
24	50	4,25	1,5	60	83,75	83,1
25	55	4,25	1	30	82,12	81,6
26	45	4,25	1,5	45	77,77	74,3
27	55	4,25	0,5	45	73,14	72,87
28	50	4,25	1	45	82,98	79,2
29	50	4,25	1	45	83,97	85,6

Source: Authors, (2025).

Table 3: ANOVA on response surface quadratic model for esterification process.

Source	Sum of Squares	df	Mean Square	F Value	p-value
Model	428.33	14	30.60	6.65	0.0005
A-Temp.	5.08	1	5.08	1.10	0.3112
B-Molar Ratio	22.68	1	22.68	4.93	0.0434
C-H_2SO_4 Conc.	113.60	1	113.60	24.70	0.0002
D-Time	19.25	1	19.25	4.18	0.0601
AB	1.27	1	1.27	0.28	0.6081
AC	7.34	1	7.34	1.60	0.2270
AD	1.22	1	1.22	0.27	0.6147
BC	53.41	1	53.41	11.61	0.0042
BD	23.22	1	23.22	5.05	0.0413
CD	5.71	1	5.71	1.24	0.2837
A*A	99.40	1	99.40	21.61	0.0004
B*B	5.17	1	5.17	1.12	0.3068
C*C	28.62	1	28.62	6.22	0.0257
D*D	18.39	1	18.39	4.00	0.0653
Residual	64.38	14	4.60		
Lack of Fit	63.57	10	6.36	31.14	0.0023
Pure Error	0.82	4	0.20		
Cor Total	492.71	28			
Other Statistics:					
Std. Dev. = 2.14		R-Squared = 0.8693			
Mean = 81.83		Adj R-Squared = 0.7387			
C.V. % = 2.62		Pred R-Squared = 0.2543			
PRESS = 367.42		Adeq Precision = 11.297			

Source: Authors, (2025).

The p-value serves as a tool to gauge the significance of each regression coefficient, including the interaction effects of cross-products. When it comes to the model terms, a p-value less than 0.05 indicates the significant influence of these parameters. The quadratic regression model, after excluding non-significant factors, formulated with the determined coefficients based on the coded parameters, is presented in Equation (5):

$$\%FAEE = +83.25 - 1.37B + 3.08C - 3.65BC - 2.41BD - 3.91A^2 - 2.10C^2 \quad (5)$$

A low coefficient of variation (CV= 2.62%) indicates the reliability of the fitted model's results. The R^2 value of 0.87, which reflects the relationship between predicted and actual values, suggests that approximately 87% of the variation in FAEE production is attributed to the independent variables, while only 13% of the total variation remains unexplained by the model, as depicted in Figure 1 (The predicted yields range from 73.14% to 92.85%, with actual yields closely aligning, indicating potential robustness of the predictive model employed). The Model F-value of 6.65 indicates the model's significance. There is a mere 0.05% chance that such a large Model F-Value could occur due to random factors [58]. The low value of pure error (0.82) signifies the excellent consistency of the data and a dependable coefficient of determination (R^2= 0.87) [59]. Additionally, as evident in Table 2, the predicted %FAEE values from the model closely aligned with the experimental values.

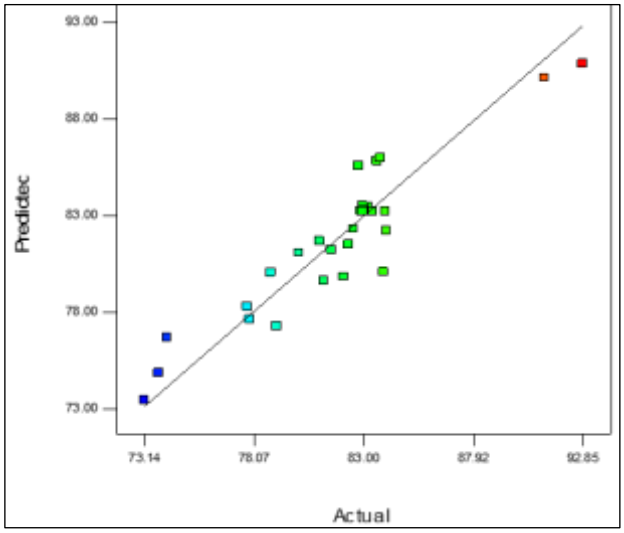

Figure 1: Plot of Predicted versus actual fatty acid ethyl esters yield (%).
Source: Authors, (2025).

Figure 2 is a showcasing of the regression equation (5). It provides a visual representation of how the dependent and independent variables relate to each other while holding specific parameters constant. The response surface analysis reveals a clear trend: yield increases significantly with rising temperatures and reduced catalyst concentrations up to a certain limit, after which diminishing returns are observed. This behavior highlights the presence of an optimal temperature, as excessive heat can result in: the evaporation of methanol, which consequently lowers the reaction rate [23]; the formation of unwanted by-products or the hydrolysis of oil: leading to an increase in the FFA value and ultimately reducing the conversion yield. Figure 2(a) displays both a 3D plot and a contour plot representing the interaction effects between alcohol molar ratio and reaction temperature on %FAEE yield. The FAEE yield increases as the temperature rises to 50ºC, reaching its peak at 0.63 mol of alcohol, after which further increases in alcohol and temperature do not substantially improve the yield. The contour plot reveals that over 85% of FAEE is produced within the range of 0.52-0.85 mol of alcohol and 48-53ºC temperature. However, at higher alcohol concentrations, there's a reduction in yield, likely due to increased glycerol solubility, making it challenging to separate the ester layer [60]. Figure 2(b) explores the impact of time and alcohol concentration on FAEE yield.

At low alcohol concentrations, the FAEE yield steadily increases with time, whereas at high alcohol concentrations, the yield decreases slightly with time. Similar trends were reported by Gupta et al. [39] in their optimization study of FAME production from a mixture of edible and non-edible vegetable oils. Additionally, at the minimum time point, an increase in FAEE yield is observed with alcohol concentration starting from 4.25 mol, with the maximum yield achieved near the maximum time and a 0.5:1 alcohol-to-oil molar ratio due to the positive linear effect of reaction time. Rapid transesterification reactions, which occur in a short time, contribute to this behavior [34, 39]. Figure 2(c) presents the effects of time and temperature on conversion yield. It shows that as the temperature increases up to approximately 52ºC, the FAEE yield increases and then starts declining.

The maximum yield is attained near the maximum time and at 50ºC. Achieving a %FAEE of over 85% is feasible when employing a reaction temperature between 50 and 52.5 ºC and a reaction time ranging from 56 to 60 minutes. In Figure 2(d), the interaction effects of temperature and catalyst concentration on conversion yield are examined. Although the interaction effect is not significant, the variation appears to exhibit a peak, resulting in a nearly constant %FAEE yield at higher acid concentration ratios and medium-range temperatures. The results indicate that at a low catalyst concentration, the yield increases from 75% to 82% with increasing temperature. This trend reflects the fact that the transesterification reaction rate accelerates with rising temperature, consistent with observations in the literature [61] regarding the optimization of biodiesel production through transesterification of soybean oil with ethanol and NaOH. Figure 2(e) shows the response for the interaction between acid catalyst concentration and time. FAEE yield increases with both catalyst concentration and time, ranging from 30 to 60 minutes. The contour plot reveals that over 85% of FAEE is produced with catalyst concentrations between 0.96 and 1.5 wt% and reaction times ranging from 52.5 to 60 minutes. Lastly, Figure 2(f) presents the response for the interacting factors of catalyst concentration and ethanol-to-oil molar ratio. The effect of the ethanol-to-oil molar ratio on FAEE yield is somewhat pronounced in the presence of H_2SO_4. This suggests that at a low ethanol-to-oil molar ratio, increasing the acid concentration boosts FAEE yield. It was observed that a yield of over 90% for FAEE could be achieved with a high level of acid catalyst concentration and a low ethanol-to-oil molar ratio.

The model's accuracy was verified by analyzing residual plots, which depict the differences between actual and predicted response values (biodiesel yield). As seen in Figure 3, an analysis of the residual plots revealed no noticeable trends or patterns, indicating that the model is well-fitted. The even distribution of residuals across all predicted value levels supports the assumptions of independence and

constant variance. Additionally, the lack of outliers further confirms that the model's assumptions are upheld, thereby reinforcing the reliability of the analysis results. In Figure 3(a), a straight line closely aligns with the normal plot of residuals, indicating a good fit [62], [63]. This suggests that the errors follow a normal distribution and are not significant. Figure 3(b) shows a random pattern of residuals versus run order, signifying model accuracy [62], [64]). Figure 3(c) displays a structure-less plot of residuals versus the predicted response, suggesting that the model is adequate and does not violate the assumptions of independence or constant variance [65].

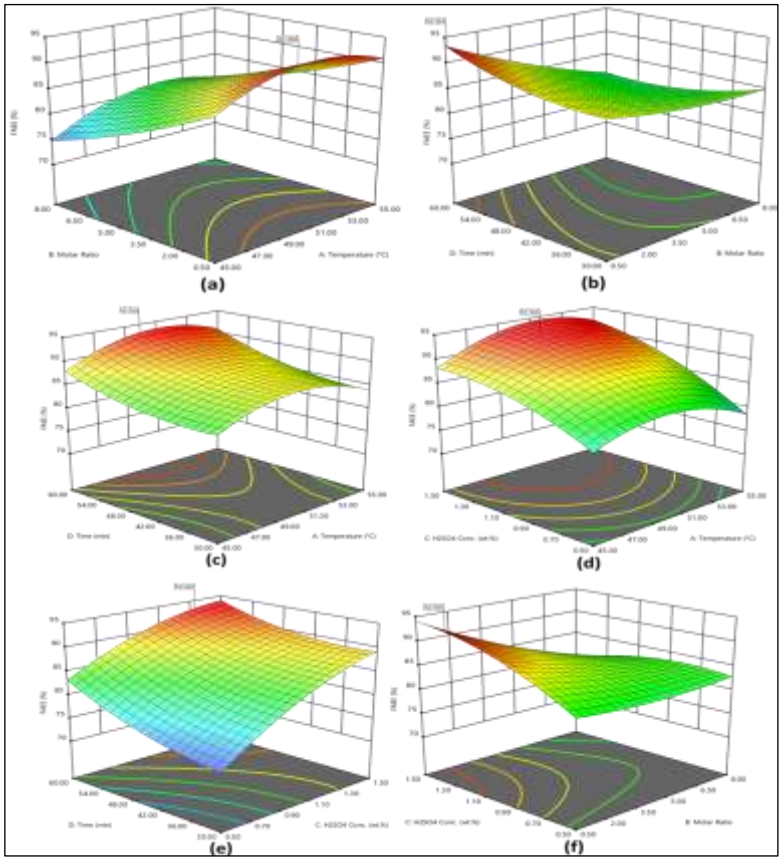

Figure 2: Response surface representation of the effect of process parameters on fatty acid ethyl esters Yield in the esterification step.
Source: Authors, (2025).

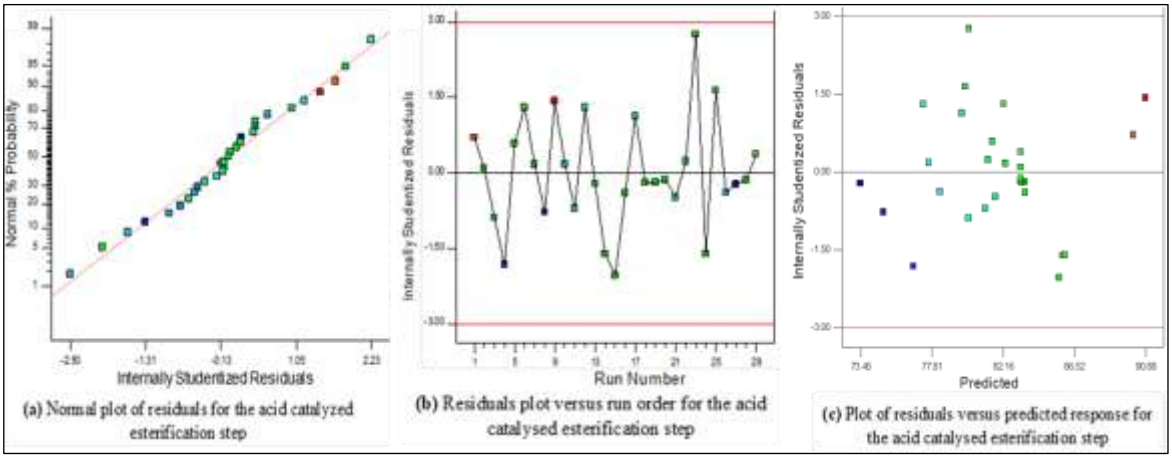

Figure 3: Residual Plots illustration for esterification step.
Source: Authors, (2025).

Table 4 illustrates the coefficients of the various factors and their impact on the oil esterification response. By examining the signs of the coefficients in model equation (5), it becomes evident that certain factors have significant effects on %FAEE:

- Factors B (3.14%) and C (15.88%) exhibit a positively significant linear influence on %FAEE by lowering the FFA.
- The interaction between BC and BD also has a notable impact on %FAEE.
- Conversely, significant quadratic terms such as AA (25.59%) and CC (7.38%) exert adverse effects, increasing the FFA hence, reducing the FAEE yield.

In the esterification process of the hybrid oil, the most influential terms, ranked in decreasing order, are as follows: AA (25.59%, quadratic term related to temperature), BC (22.30%, representing the Ethanol ratio/H_2SO_4 concentration), C (15.88%, H_2SO_4

concentration), BD (9.72%, Ethanol ratio/Time), and CC (7.38%, quadratic term linked to H_2SO_4 concentration). These five terms collectively contribute to 80.87% of the esterification of the hybrid oil.

Table 4: Factors coefficients and weights on the hybrid oil esterification response.

Factors	Coefficient	Coefficient square	%effect
Constant	83.25		
A	0.65	0.4225	0.707141375
B	-1.37	1.8769	3.141381411
C	**3.08**	**9.4864**	**15.87745784**
D	1.27	1.6129	2.699522659
AB	0.56	0.3136	0.524874639
AC	1.36	1.8496	3.095689199
AD	0.55	0.3025	0.506296487
BC	**-3.65**	**13.3225**	**22.29796678**
BD	**-2.41**	**5.8081**	**9.721059925**
CD	-1.2	1.44	2.41013865
AA	**-3.91**	**15.2881**	**25.58780604**
BB	0.89	0.7921	1.325743628
CC	**-2.1**	**4.41**	**7.381049615**
DD	1.68	2.8224	4.723871754
$\sum \beta_I^2 = 59.7476$			

Source: Authors, (2025).

III.1.2. TRANSESTERIFICATION PROCESS

Based on the preliminary investigations mentioned above, the BBD was employed to examine the impact of KOH concentration, ethanol-to-oil molar ratio, time, and temperature on %FAEE. Table 5 displays the experimental results alongside the predicted values for %FAEE, as well as the conversion yield, at the designated points.

Reviewing Table 5, it becomes apparent that the predicted %FAEE values from the model closely matched the experimental values. The %FAEE and % Yield exhibited variations ranging from 69.35% to 92.16% and 82.16% to 95.66%, respectively. The highest %Yield and %FAEE values were observed within a medium temperature range, at moderate catalyst concentrations, low ethanol-to-oil molar ratios, and extended reaction times. Conversely, the lowest values were recorded under high-temperature conditions, elevated KOH concentrations, and within the medium range for ethanol-to-oil molar ratios and reaction times.

Table 5: BBD matrix with four variables for the transesterification process.

Run	Temp. (°C)	Ethanol molar ratio	KOH Conc. (wt,%)	Time (min)	%FAEE from expt.	%FAEE from Model	Yield (%)
1	65.00	9.50	1.25	60.00	84.13	83.12	93.26
2	65.00	3.50	1.25	60.00	92.16	89.35	95.66
3	65.00	6.50	0.50	60.00	80.60	82.76	87.89
4	65.00	6.50	1.25	45.00	81.35	82.11	90.12
5	50.00	9.50	1.25	45.00	80.12	83.98	86.21
6	65.00	6.50	1.25	45.00	80.97	78.17	90.32
7	80.00	6.50	2.00	45.00	69.35	77.7	82.16
8	65.00	6.50	2.00	30.00	80.79	79.16	87.89
9	65.00	6.50	1.25	45.00	81.07	83.1	89.71
10	65.00	3.50	0.50	45.00	89.42	86.67	95.07
11	65.00	6.50	1.25	45.00	81.21	78.12	89.45
12	65.00	3.50	1.25	30.00	91.10	89.35	95.51
13	80.00	9.50	1.25	45.00	84.29	82.16	94.32
14	65.00	9.50	1.25	30.00	83.25	81.90	89.56
15	80.00	6.50	1.25	60.00	81.75	81.00	89.45
16	80.00	6.50	1.25	30.00	81.55	81.41	88.67
17	65.00	9.50	0.50	45.00	83.19	82.74	88.58
18	65.00	9.50	2.00	45.00	83.13	84.00	89.23
19	65.00	6.50	0.50	30.00	81.53	82.7	89.62
20	65.00	6.50	1.25	45.00	81.21	79.02	89.38
21	50.00	6.50	0.50	45.00	82.14	82.1	90.28
22	50.00	3.50	1.25	45.00	87.68	85.6	91.33
23	50.00	6.50	1.25	60.00	81.56	82.15	89.81
24	65.00	3.50	2.00	45.00	81.88	80.40	90.39
25	50.00	6.50	2.00	45.00	82.56	84.04	90.58
26	65.00	6.50	2.00	60.00	80.69	78.33	87.69
27	80.00	3.50	1.25	45.00	84.70	85.48	93.26
28	50.00	6.50	1.25	30.00	81.85	84.04	90.13
29	80.00	6.50	0.50	45.00	82.17	83.54	90.37

Source: Authors, (2025).

To predict the full quadratic model for %FAEE related to the operational parameters in the second esterification step, regression coefficients, and constants were obtained, as displayed in Table 6. The R^2 was found to be 84.9%. Utilizing these coefficients, the predicted full quadratic model for %FAEE is represented in Equation. (6).

$$\%FAEE = 81.16 - 2.40B - 1.72C - 3.31AC + 4.57B^2 \quad (6)$$

The importance of each coefficient in equation (6) was assessed using the P-value, as presented in Table 6.

Table 6: ANOVA on Response Surface Quadratic Model for transesterification.

Source	Sum of Squares	df	Mean Square	F Value	p-value
Model	386.37	14	27.60	5.62	0.0013
A-Temp.	12.20	1	12.20	2.48	0.1373
B-Ethanol to oil molar ratio	69.30	1	69.30	14.11	0.0021
C-KOH Conc.	35.48	1	35.48	7.22	0.0177
D-Time	0.058	1	0.058	0.012	0.9153
AB	12.76	1	12.76	2.60	0.1294
AC	43.84	1	43.84	8.92	0.0098
AD	0.058	1	0.058	0.012	0.9148
BC	13.97	1	13.97	2.84	0.1139
BD	8.742E-003	1	8.742E-003	1.780E-003	0.9669
CD	0.17	1	0.17	0.035	0.8543
A^2	7.83	1	7.83	1.59	0.2273
B^2	135.38	1	135.38	27.56	0.0001
C^2	12.44	1	12.44	2.53	0.1339
D^2	15.68	1	15.68	3.19	0.0957
Residual	68.78	14	4.91		
Lack of Fit	68.70	10	6.87	333.17	< 0.0001
Pure Error	0.082	4	0.021		
Cor Total	455.14	28			
Other Statistics:					
Std. Dev. = 2.22		R-Squared = 0.8489			
Mean = 82.67		Adj R-Squared = 0.6978			
C.V. % = 2.68		Pred R-Squared = 0.1303			
PRESS = 395.82		Adeq Precision = 11.102			

Source: Authors, (2025).

Considering the linear impact, it was determined that both the ethanol-to-oil molar ratio and the KOH concentration held significance at a 5% significance level. Regarding the quadratic effect, only the ethanol-to-oil molar ratio exhibited significance. However, the interaction effect between temperature and KOH concentration was also found to be significant at a 5% level. Therefore, this interaction term played a crucial role in the final percentage of FAEE. Similarly, Gupta et al. [39] discovered an interaction effect between catalyst concentration and temperature in the production of biodiesel from a mixture of edible and nonedible vegetable oils using an alkaline-catalyzed process. In contrast, Yuan et al.[58] observed a minimal interaction effect between catalyst concentration and temperature in the production of biodiesel from waste rapeseed oil using the same alkaline-catalyzed process.

A low coefficient of variation (CV=2.68%) suggests that the fitted model's results are reliable. The low pure error value (0.082) indicates excellent data regeneration and a dependable coefficient of determination (R^2=0.85), demonstrating a strong correlation among the independent variables. Furthermore, the Model F-value of 5.62 suggests the model's significance, with only a 0.13% chance that such a large "Model F-Value" could occur due to noise [66], [67]. "Adeq Precision" measures the signal-to-noise ratio, and a value of AP > 4 indicates adequate signal quality, making the model suitable for navigating the design space [68], [69]. The R^2 value (0.85), representing the relationship between predicted and actual values, indicates that 85% of the variation in FAEE production can be attributed to the independent variables, leaving only 15% unexplained by the model [58], [59], as depicted in Figure 4.

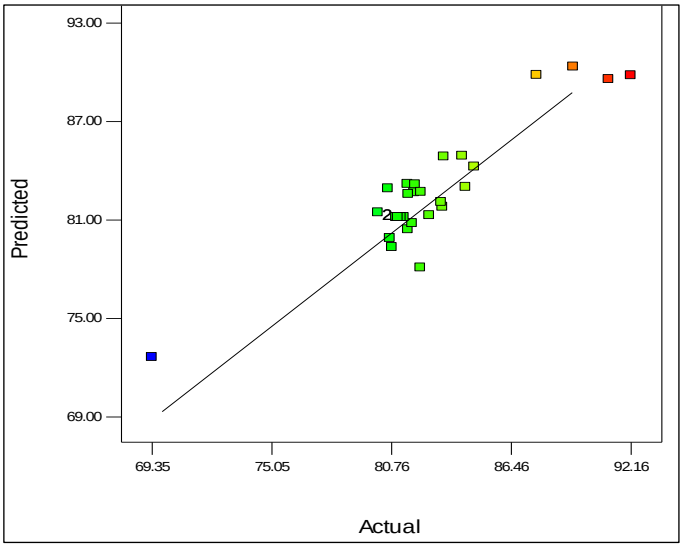

Figure 4: Plot of predicted values and actual values for transesterification.
Source: Authors, (2025).

Table 7 displays the coefficients of various factors and their impact on the oil transesterification response. From the signs of the coefficients in model equation (6), it is evident that term B (10.69% - Ethanol/oil molar ratio) had a significant negative linear effect on %FAEE. Additionally, term AC (20.34% - Temperature/KOH concentration) exhibited a significant negative interaction effect on %FAEE. However, significant quadratic terms, specifically BB (38.77% - ethanol/oil molar ratio), had positive effects that boosted FAEE yield. These three terms collectively contributed to 69.8% of the hybrid oil transesterification.

Table 7: Factors coefficients and weight on transesterification response.

Factors	Coefficient	Coefficient square	%effect
Constant	81.16		
A	-1.01	1.0201	1.893883486
B	**-2.4**	**5.76**	**10.69382304**
C	-1.72	2.9584	5.492466332
D	0.069	0.004761	0.008839113
AB	1.79	3.2041	5.948624721
AC	**-3.31**	**10.9561**	**20.34072822**
AD	0.12	0.0144	0.026734558
BC	1.87	3.4969	6.492227392
BD	0.047	0.002209	0.004101155
CD	0.21	0.0441	0.081874583
AA	-1.1	1.21	2.246445464
BB	**4.57**	**20.8849**	**38.77420568**
CC	-1.38	1.9044	3.535645241
DD	1.55	2.4025	4.460401015
$\sum \boldsymbol{\beta_I^2} = \mathbf{53.86287}$			

Source: Authors, (2025).

The relationships between the analyzed variables for different parameters are presented in Figure 5. Figure 5(a) depicts a 3D plot and a contour plot illustrating the interaction effects between the ethanol/oil molar ratio and reaction temperature on the %FAEE yield. The FAEE yield increases as the temperature and ethanol/oil molar ratio decrease. The contour plot's shape reveals that more than 89% of FAEE was produced at lower temperatures and ethanol molar ratio values. This observation aligns with the findings of Charoenchaitrakool & Thienmethangkoon [34], who produced FAME from waste frying oil and noted a similar trend. Figure 5(b) illustrates the effects of time and alcohol concentration on FAEE yield.

Since there is no interaction between these parameters, the contour curve appears relatively circular, as noted by Yuan et al.[58]. Maximum %FAEE can be obtained by increasing the reaction time while decreasing the ethanol concentration. More than 89% FAEE is observed near the maximum reaction time and a 3.5:1 ethanol/oil molar ratio. Figure 5(c) shows the effects of time and temperature on conversion yield. An increase in FAEE yield is observed with temperatures up to around 63ºC, especially near the maximum and minimum times. A %FAEE of over 82% can be achieved when using a reaction temperature in the range of 50 to 63ºC and a reaction time in the range of 30-34 minutes or 56-60 minutes. Figure 5(d) indicates the effects of temperature and catalyst concentration on the conversion yield. The variation suggests that a maximum and relatively steady %FAEE can be obtained at low alkali concentrations and a high-temperature range.

The results show that about 82% of FAEE can be obtained near the maximum temperature with approximately 0.56 wt.% KOH. Figure 5(e) illustrates the response for the interacting factors of alkali catalyst concentration and time. An increase in FAEE yield is observed with KOH concentration up to approximately 1.32 wt.% near the maximum and minimum times. A %FAEE of more than 82% can be achieved when using a reaction KOH concentration in the range of 0.5 to 1.25 wt% and a reaction time in the range of 30-35 minutes or 55-60 minutes. Figure 5(f) presents the response for the interacting factors of catalyst concentration and ethanol to oil molar ratio. The rate of FAEE yield increase is noticeable with a simultaneous decrease in catalyst concentration and ethanol/oil molar ratio. However, it was found that more than 89% FAEE yield could be achieved at low levels of KOH catalyst concentration and low ethanol-to-oil molar ratios. Examination of Fig 5 reveals distinct trends in FAEE yield, showing a steady increase with rising temperatures up to a critical threshold of approximately 65°C. Beyond this point, the yield stabilizes and, in some cases, declines, suggesting a complex interaction of factors as seen in Table 7.

This behavior may result from thermal degradation of oil or the formation of undesirable byproducts at higher temperatures, reducing overall efficiency. Additionally, an anomaly is observed at higher catalyst concentrations (above 2.0%), where yield fails to increase proportionally with catalyst addition. This inconsistency points to possible reaction limitations or side reactions, such as soap formation, that may hinder efficiency. These non-linear relationships highlight the need for further investigation to identify the optimal operating conditions for these parameters, as such insights could lead to significant improvements in biodiesel production efficiency. Interestingly, the analysis also uncovers an unexpected interaction between catalyst concentration and reaction time.

Evidence suggests that higher catalyst levels may reduce the benefits of extended reaction durations, potentially due to an inhibitory effect of excess catalyst. This challenges the conventional assumption that "more is better" in catalyst usage. These findings call for a reassessment of the balance between catalyst concentration and reaction time to optimize yield. Yet, exploring the mechanisms behind catalyst behavior under different conditions may offer an opportunity to refine transesterification processes, paving the way for more efficient biodiesel production strategies.

The model's accuracy was assessed using residual plots, which compare actual and predicted %FAEE yield values. As shown in Fig 6, the residuals exhibit a random distribution with no discernible patterns, indicating that assumptions of homoscedasticity and normality are met. The consistent spread of residuals suggests reliable predictions across input values. However, a few data points deviate significantly, possibly representing outliers caused by experimental errors, feedstock quality variations, or other factors. For instance, elevated impurities in a feedstock batch could skew results. These deviations highlight the need for further investigation to determine their effect on the model's accuracy and biodiesel yield. In Fig 6(a), the analysis of residuals revealed no statistical issues, as the errors in the response values closely followed a normal distribution. The plot of residuals versus run order in Fig 6(b) displayed random patterns, indicating good model accuracy. Furthermore, Fig 6(c), the plot of residuals versus predicted response, exhibited a structureless pattern, suggesting that the model is adequate and does not violate the assumptions of independence or constant variance.

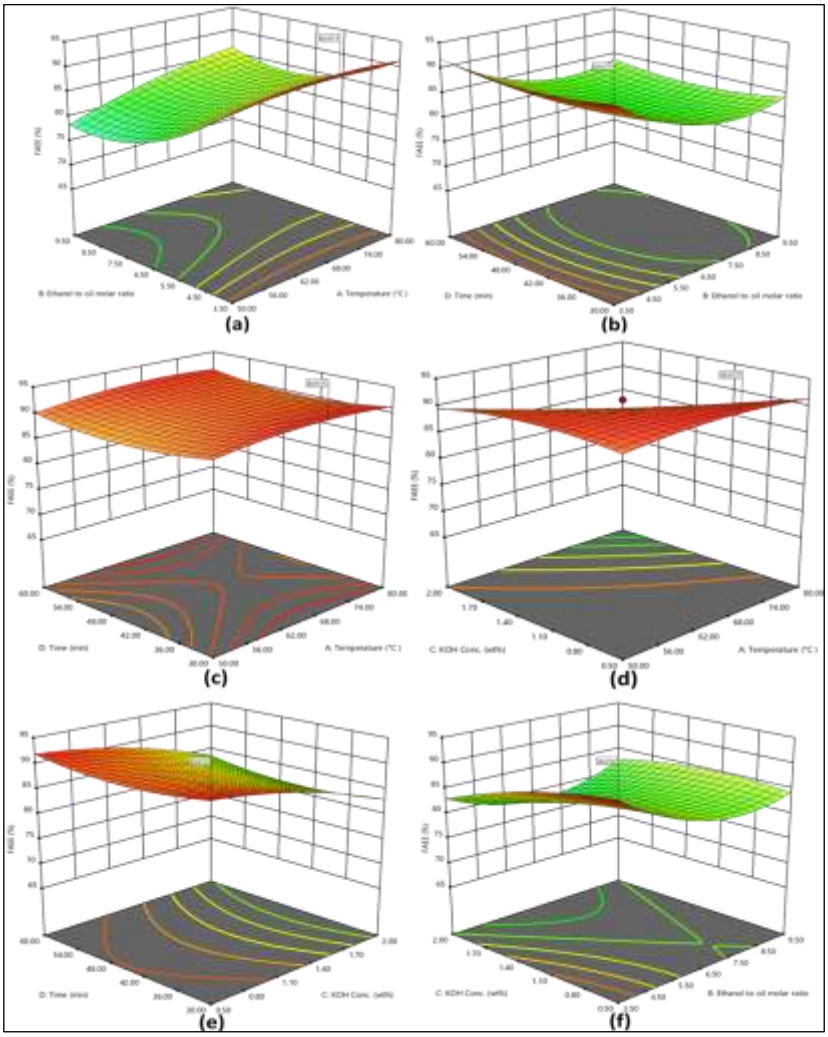

Figure 5: Response surface representation of the effect of process parameters on FAEE yield in the transesterification step.
Source: Authors, (2025).

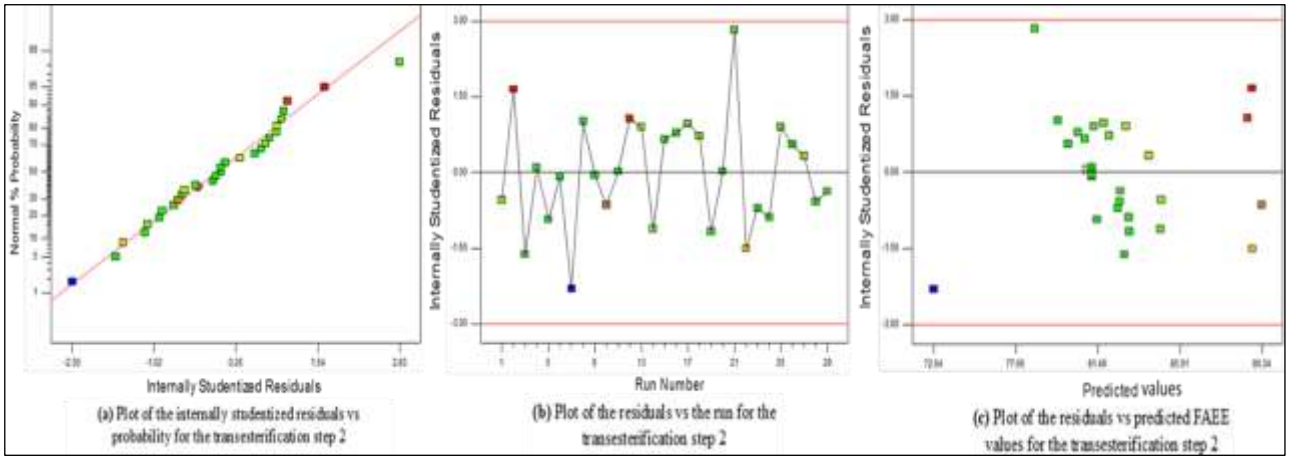

Figure 6: Residuals Plots illustration for the transesterification step.
Source: Authors, (2025).

III.2 OPTIMIZATION OF REACTION PARAMETERS AND MODELS VALIDATION

Implementing the global desirability function method, a non-zero value indicates that all responses simultaneously fall within the desirable range as is appears on Figure 7 for both; the esterification and the transesterification steps. Consequently, a *D* value close to 1 signifies that the combination of different criteria is globally optimal since the response values closely align with target values.

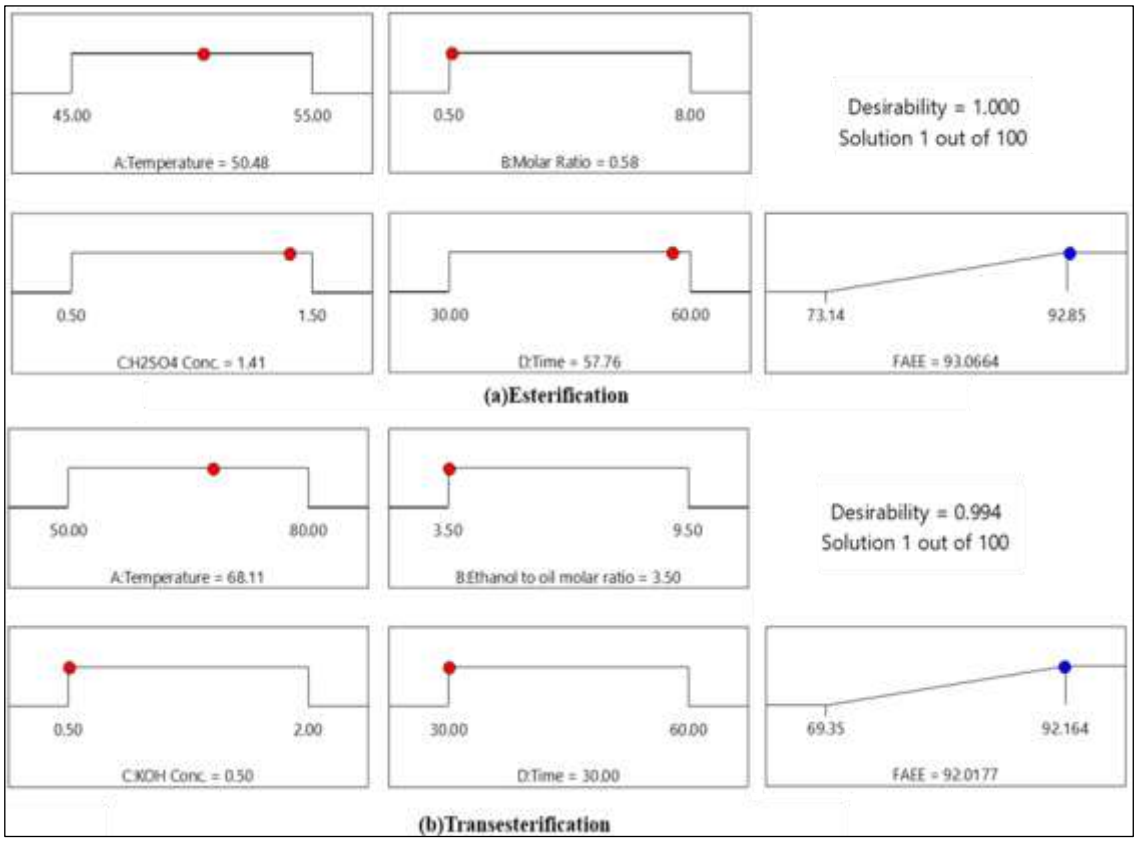

Figure 7: Ramp function desirability representation for the dual-phase process.
Source: Authors, (2025).

In the first step (esterification), three optimal conditions are presented (Table 8), with the highest desirability value (D = 1) achieved under specific parameters. These parameters include an alcohol-to-oil molar ratio of 1.28:1, a reaction time of 59.87 minutes, a reaction temperature of 51.72ºC, and acid catalyst amount of 1.46 wt.%. The second step (transesterification) also presents three optimal solutions (Table 9), with the first group yielding a desirability value of 0.99. The best compromise in this step includes an ethanol-to-oil molar ratio of 3.5:1, a reaction time of 30 minutes, a reaction temperature of 68.84ºC, and a KOH catalyst amount of 0.52 wt.%. The corresponding response surface plots, illustrating the best compromise (for both steps), is depicted in Figure 8. Predicted %FAEE at these conditions is 91.96%, and verification experiments closely aligned with this prediction, yielding 90.53±0.28%. Moreover, with AADM values < 10%; the quadratic models employed in the various steps are considered accurate and reliable for predicting %FAEE, with a small percentage error of 1.55% between experimental and predicted results.

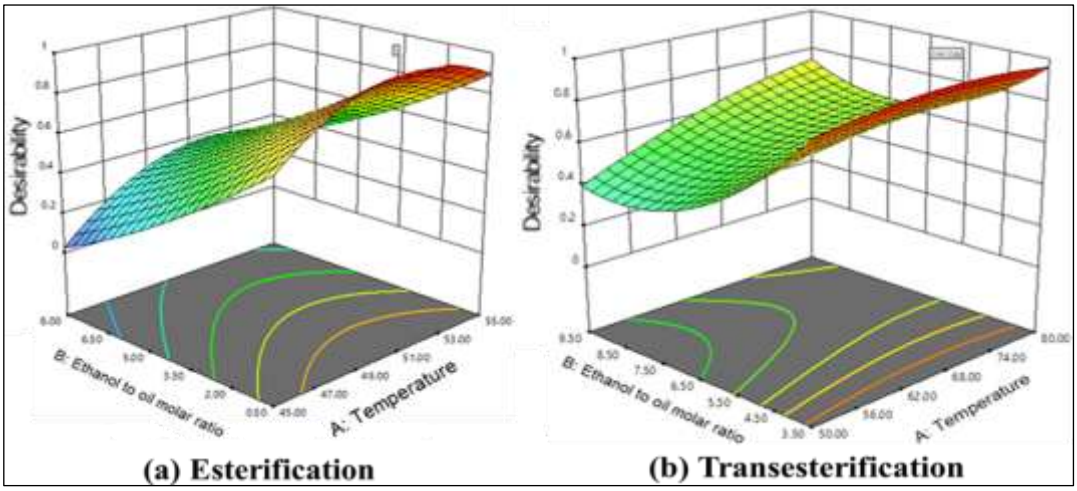

Figure 8: 3D representation of the overall desirability.
Source: Authors, (2025).

Table 8: Criteria for numerical optimization of the acid catalyzed esterification step with desirability function approach for hybrid oil biodiesel production.

Parameters	Goal	Lower Limit	Upper Limit	Lower Weight	Upper Weight	Importance
Temperature (°C)	In range	45	55	1	1	3
Ethanol to oil molar ratio	In range	0.5	8	1	1	3
H_2SO_4 Concentration (wt.%)	In range	0.5	1.5	1	1	3
Time (min)	In range	30	60	1	1	3
FAEE (%)	Maximize	73.14	92.85	1	1	3

Solutions:

Number	Variables				Response			
					% FAEE			
	Temperature	Ethanol Molar Ratio	H_2SO_4 Conc.	Time	Exp	Pred	Desirability	
1	51.72	1.28	1.46	59.87	94.57±0,76	93.25	1	*Selected*
2	49.96	0.73	1.36	59.49	---	93.07	0.97	
3	53.43	0.66	1.43	59.7	---	93.99	0.95	
% Error				-1.42				
AADM obtained 0.0802								
Exp =Experimental *Pred = Predicted* *AADM = Absolute analysis average deviation*								

Source: Authors, (2025).

Table 9: Criteria for numerical optimization of the transesterification conditions with desirability function approach for the hybrid oil biodiesel production.

Parameters	Goal	Lower Limit	Upper Limit	Lower Weight	Upper Weight	Importance
Temperature (°C)	In range	50	80	1	1	3
Ethanol to oil molar ratio	In range	3.5	9.5	1	1	3
KOH Concentration (wt.%)	In range	0.5	2	1	1	3
Time (min)	In range	30	60	1	1	3
FAEE (%)	Maximize	69.35	92.164	1	1	3

Solutions:

Number	Variables				Response			
					% FAEE			
	Temperature	Ethanol Molar Ratio	KOH Conc.	Time	Exp	Pred	Desirability	
1	68.84	3.5	0.52	30	90.53±0.28	91.96	0.991	*Selected*
2	64.25	3.51	0.51	30	---	91.90	0.988	
3	69.21	3.5	0.5	60	---	91.89	0.988	
% Error				1.55				
AADM obtained 0.0094								
Exp =Experimental *Pred = Predicted* *AADM = Absolute analysis average deviation*								

Source: Authors, (2025).

III.3 COMPARISON OF THE STUDY WITH EXISTING LITERATURE

Table 10 provides a comparison of the present study with existing literature. The data indicate that lower catalyst concentrations, such as 0.52 wt.% KOH falls within the typical range for transesterification reactions (0.5%–1.5% by weight) as reported by Gupta et al. [39]. Additionally, the optimal conditions achieved in this study are comparable to those reported by Betiku et al. [56]. However, the biodiesel yield of 90.53% is lower than the results reported by Harisha et al. [44], Suherman et al.[70], and Kusumo et al.[46]. These differences may be attributed to two primary factors: the unique properties of the feedstock oil, such as its chemical composition, kinematic viscosity, alcohol solubility, and the specific procedures and reactants used in the transesterification process. In contrast, the yield of 83.20% obtained using a heterogeneous catalyst in Brihaspati et al. [12] stands out as an outlier, suggesting that variations in feedstock and processing conditions can result in lower yields. This emphasizes the critical role of selecting appropriate feedstock and optimizing operational parameters. From a practical perspective, the high yield achieved in this study with minimal catalyst usage and a shorter processing time demonstrates the potential for industries to enhance the economic feasibility of biodiesel production by adopting similar optimized conditions.

Table 10: Comparison of the study with literature.

Optimum conditions	**Feedstock (mixture)**	**Yield (%)**	**Reference work**
KOH 0.52wt.%; 3.5:1; 69 ºC; 400rpm; 30min	Shea butter, Neem oil, and Waste kitchen oil	90.53	Present work
Heterogeneous catalyst 5 wt%; 9:1; 60ºC; 800rpm; 130min	Waste cooking oil, *Ricinus* communis oil and *Melia azedarach* oil	83.20	[12]
NaOH 61.2 wt%; 6:1; 4 °C; 500rpm; 75min	Pongamia oil, waste cooking oil and animal fat	97.76	[44]
KOH 0.5wt.%;10:1; 60ºC; 90min	Waste Cooking Oil and *Schleichera oleosa* Oil	92.4	[70]
KOH 1 wt %; 9 :1; 50ºC; 400 rpm ; 90min	Jatropha oil, Palm oil and *karanja* oil	-	[50]
KOH 0.7% wt; 42%; 50.64 min	*Sterculia foetida* and rice bran oil	98.93	[46]
KOH 1.89 wt.%; 8.83:1; 43.5 ºC; 58.36min	Palm oil, linseed oil, Karanj oil and thumba oil	96.4	[39]
KOH 1.4 wt.%; 7.5:1; 65 ºC; 500rpm; 60 min	Waste cooking oil (soybean and sunflower)	99.3	[71]
KOH 1wt.%; 6:1; 60 ºC; 600rpm; 60min	Palm kernel oil and groundnut oil	86.56	[72]

Source: Authors, (2025).

III.4 QUANTITATIVE ANALYSIS OF FATTY ACID ETHYL ESTER CONTENT

The GC-MS chromatogram (Figure 9) from the FAEE analysis displays multiple distinct and well-defined peaks, each representing a specific fatty acid. Prominent peaks associated with palmitic acid (C16:0) and oleic acid (C18:1) highlight their significance in the biochemical composition of the feedstock. These fatty acids are renowned for their advantageous properties in biodiesel production, such as low viscosity and high cetane numbers. The detection of ethyl esters in the chromatogram confirms the effectivity of the transesterification process, a key step in converting triglycerides into biodiesel. The chromatogram reveals trends suggesting preferential formation of certain fatty acids during transesterification. For example, a significant peak at a retention time of 12.5 minutes likely corresponds to a dominant fatty acid, reflecting its reactivity under the experimental conditions. Such patterns offer insights into the mechanistic pathways of transesterification and inform future optimization efforts.

In contrast, smaller peaks scattered across the chromatogram represent minor fatty acid components, underscoring the complexity of the mixture and the intricacies of the transesterification process. These minor components can influence biodiesel's physical and chemical properties, emphasizing the importance of considering the entire fatty acid profile when formulating biodiesel. The predominant fragment ions of the resultant fatty acid ethyl esters, along with other noteworthy compounds, have been documented in Table 11. Our analysis reveals that the primary ethyl ester constituents obtained are as follows: (E)-9-Octadecenoic acid ethyl ester, constituting 65.3% of the biodiesel and possessing a retention time (RT) of 23.6 minutes, serves as the predominant component of the biodiesel. Ethyl 13-methyltetradecanoate, representing 11.49% of the composition and with an RT of 24.6 minutes, emerges as the second major constituent detected. Following closely is 9,12-Octadecadienoic acid ethyl ester, accounting for 7.04% of the composition with an RT of 23.3 minutes.

Hexadecanoic acid ethyl ester, comprising 5.62% of the mixture and exhibiting an RT of 18.1 minutes, is another noteworthy component. Additionally, Diisooctyl phthalate, constituting 3.33% of the biodiesel and having an RT of 36.4 minutes, is observed. This last component, recognized as a plasticizer, may potentially be a contaminant originating from the plastic container employed in the storage and distribution of vegetable oils [73],[74]. Regardless of the source of triglycerides, biodiesel produced through transesterification primarily consists of fatty acid chains with even numbers of carbon atoms. While biodiesel derived from various vegetable oils and animal fats exhibits a multitude of distinct fatty acid ester (FAE) species, a typical biodiesel fuel is typically dominated by a select few species [75]. The major ethyl ester components identified in our study, correspond to the frequently encountered FAEs in biodiesel. [39],[75],[76].

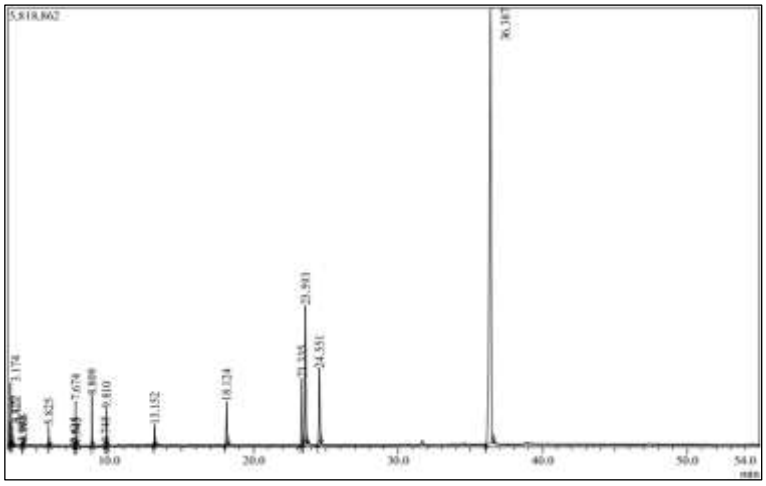

Figure 9: GC-MS Chromatogram of obtained FAEE.
Source: Authors, (2025).

Table 11: The chemical composition of the FAEE as per the GC-MS results

RT (min)	Compounds identified	Molecular formula	Molecular Weight	Area (%)
3.122	Ethylbenzene	C_8H_{10}	106	0.36
3.995	1-Decene	$C_{10}H_{20}$	140	0.05
4.066	Undecane	$C_{11}H_{24}$	156	0.06
5.825	1-Dodecene	$C_{12}H_{24}$	168	0.40
7.635	4-Undecene, 3-methyl-, (Z)-	$C_{12}H_{24}$	168	0.05
7.674	1-Tetradecene	$C_{14}H_{28}$	196	0.96
7.745	Tridecane, 2-methyl-	$C_{14}H_{30}$	198	0.06
8.809	Phenol, 2,4-bis(1,1-dimethylethyl)-	$C_{14}H_{22}O$	206	1.38
9.745	7-Hexadecene, (Z)-	$C_{16}H_{32}$	224	0.08
9.810	E-15-Heptadecenal	$C_{17}H_{32}O$	252	1.16
13.152	Trifluoroacetic acid, pentadecyl ester	$C_{17}H_{31}F_3O_2$	324	1.00
18.124	Hexadecanoic acid, ethyl ester	$C_{18}H_{36}O_2$	284	5.62
23.335	9,12-Octadecadienoic acid, ethyl ester	$C_{20}H_{36}O_2$	308	7.04
23.593	(E)-9-Octadecenoic acid ethyl ester	$C_{20}H_{38}O_2$	310	65.30
24.551	Ethyl 13-methyl-tetradecanoate	$C_{17}H_{34}O_2$	270	11.04
36.387	Diisooctyl phthalate	$C_{24}H_{38}O_4$	390	3.33
RT: Retention Time				

Source: Authors, (2025).

III.5 HYBRID BIODIESEL PHYSICAL AND CHEMICAL CHARACTERISTICS

Table 12 presents the physical properties of the biodiesel produced, compared to various international standards for FAME and FAEE. The biodiesel had a pale-yellow color and its measured properties—such as viscosity, density, cloud point, flash point, cetane number, and high calorific value—aligned with biodiesel standards set by the United States, Europe, India, Brazil, and South Africa. Consequently, the biodiesel produced under optimal conditions shows great potential as a viable alternative fuel for agricultural machinery, industrial automotive and power plant applications. Except for the acid value, suggesting the need for additional pretreatment of the hybrid oil before its use in biodiesel production.

Table 12: Physical properties of the produced biodiesel compared to some international standards.

Property	**Testing method**	**Produced Biodiesel**	**ASTM D6751**	**EN 14214**	**ANP 42**	**SANS 1935**	**IS 15607**
Viscosity (mm^2/s)	ASTM D445	4.48	1.9 - 6	3.5 - 5	--	3.5 - 5	2.5 - 6
Density (kg/m^3)	ASTM D1298	862.9	--	860 - 900	--	860 - 900	860 - 900
Cetane number	Calculated	62.43	≥47	≥51	≥45	≥51	≥51
Cloud point (°C)	ASTM D2500	20	--	--	--	--	--
Flash point (°C)	ASTM D92	190	≥93	≥120	1≥00	≥120	≥120
Acid value (mgKOH/g)	AOAC	0.83	≤0.5	≤0.5	≤0.8	≤0.5	≤0.5
High calorific value (MJ/kg)	Calculated	40.88	--	≥35	--	--	--
Iodine Value ($gI_2/100$ g)	AOAC	22.5	≤ 120	--	--	--	--
Oxidation stability (hr)	Rancimat apparatus	10.12	≥3	≥ 8	--	--	--

ASTM D6751=American biodiesel standard
EN 14214= European biodiesel standard
IS 15607= Indian bio-diesel standard
ANP 42 = Brazilian biodiesel standard
SANS 1935 = South Africa biodiesel standard

Source: Authors, (2025).

IV. CONCLUSION

This research investigated the potential of a two-step transesterification process using a hybrid feedstock of Neem oil, Shea butter, and Waste kitchen oil for biodiesel production. The application of the desirability function demonstrated that the combination of Response Surface Methodology with the desirability approach represents a viable and effective solution for achieving multiresponse optimization for chemical processes. The hybrid feedstock of Neem oil, Shea butter, and Waste kitchen oil showed promise as a viable source for biodiesel production. It offers the advantage of utilizing non-traditional and waste-derived oils, promoting resource efficiency and sustainability. Two second-order polynomial models were developed to describe the two-step transesterification process, and these models demonstrated satisfactory validation based on parameters such as the coefficient of determination (R^2), the F-value, and the P-value. At an agitation speed of 400 rpm, the optimal conversion conditions were determined as follows: for the first step (esterification), a reaction time of 59.87 minutes, an ethanol-to-oil molar ratio of 1.28:1, a reaction temperature of 51.72°C, and an H_2SO_4 concentration of 1.46 wt.% of oil. Similarly, for the second step (transesterification), the optimal conditions included a reaction time of 30 minutes, an ethanol-to-oil molar ratio of 3.5:1, a reaction temperature of 68.84°C, and a KOH concentration of 0.52 wt.%.

V. AUTHOR'S CONTRIBUTION

Conceptualization: Narcisse S. Nouadjep, César Kapseu and Roland Solimando.
Methodology: Narcisse S. Nouadjep, César Kapseu and Roland Solimando.
Investigation: Narcisse S. Nouadjep, César Kapseu and Roland Solimando.
Discussion of results: Narcisse S. Nouadjep, César Kapseu and Roland Solimando.
Writing – Original Draft: Narcisse S. Nouadjep, César Kapseu and Roland Solimando.
Writing – Review and Editing: Narcisse S. Nouadjep, César Kapseu and Roland Solimando.
Resources: Narcisse S. Nouadjep, César Kapseu and Roland Solimando.
Supervision: Narcisse S. Nouadjep, César Kapseu and Roland Solimando.
Approval of the final text: Narcisse S. Nouadjep, César Kapseu and Roland Solimando.

VI. REFERENCES

[1] Farghali M, Osman AI, Chen Z, Abdelhaleem A, Ihara I, Mohamed IMA, Yap P-S, Rooney DW (2023a) Social, environmental, and economic consequences of integrating renewable energies in the electricity sector: a review. Environ Chem Lett 21(3):1381–1418. https://doi.org/10.1007/s10311-023-01587-1

[2] Maheshwari P, Haider MB, Yusuf M, Klemes JJ, Bokhari A, Beg M, Al-Othman A, Kumar R, Jaiswal AK (2022) A review on latest trends in cleaner biodiesel production: role of feedstock, production methods, and catalysts. J Clean Prod 355:131588. ARTN 131588. https://doi.org/10.1016/j.jclep ro.2022.131588

[3] Brahma S, Nath B, Basumatary B, Das B, Saikia P, Patir K, Basumatary S., 2022. Biodiesel production from mixed oils: a sustainable approach towards industrial biofuel production. Chem Eng J Adv10:100284. https://doi.org/10.1016/j.ceja.2022.100284

[4] Alalaiwat D, Khan E (2023) Current status and future scenarios of carbon capture from power plants emission: a review. Rev Environ Sci Bio-Technol 22(3):799–822. https://doi.org/10.1007/s11157- 023- 09663-2

[5] Esmaeili H., 2022. A critical review on the economic aspects and life cycle assessment of biodiesel production using heterogeneous nanocatalysts. Fuel Process Technol 230:107224. https://doi.org/10.1016/j.fuproc.2022.107224

[6] Osman, A.I., Nasr, M., Farghali, M. et al.,2024. Optimizing biodiesel production from waste with computational chemistry, machine learning and policy insights: a review. Environ Chem Lett 22, 1005–1071 (2024). https://doi.org/10.1007/s10311-024-01700-y

[7] Farghali M, Osman AI, Mohamed IMA, Chen Z, Chen L, Ihara I. et al., 2023b. Strategies to save energy in the context of the energy crisis: a review. Environ Chem Lett. https://doi.org/10.1007/s10311-023-01591-5

[8] Wang X, Huang J, Liu H., 2022. Can China's carbon trading policy help achieve Carbon Neutrality? A study of policy effects from the five-sphere integrated plan perspective. J Environ Manag 305:114357. https://doi.org/10.1016/j.jenvm an.2021.114357

[9] IEA. 2022. World energy outlook 2022, part of world energy outlook. www.iea.org/t&c/%0Ahttps://www.iea.org/reports/world-energy-outlook-2022

[10] Tan, D., Y. Wu, J. Lv, J. Li, X. Ou, Y. Meng, G. Lan, Y. Chen, and Z. Zhang. 2023. Performance optimization of a diesel engine fueled with hydrogen/biodiesel with water addition based on the response surface methodology. Energy 263:125869. DOI:10.1016/j.energy.2022.125869.

[11] Wu, T., Q. Shen, M. Xu, T. Peng, and X. Ou. 2018. Development and application of an energy use and CO2 emissions reduction evaluation model for China's online car hailing services. Energy 154:298–307. DOI:10.1016/j.energy.2018.04.130.

[12] Brihaspati Singh, Anmesh Kumar Srivastava & Om Prakash (2024). Hybrid biodiesel production from optimized novel ternary oil mixture (simplex lattice mixture design) using heterogeneous river shell catalyst. Energy Sources, Part A: Recovery, Utilization, and Environmental Effects, 46:1, 2973-2992. DOI:10.1080/15567036.2024.2310744

[13] M. Jayakumar. 2023. Biodiesel production from Argemone mexicana oil using chicken eggshell derived CaO catalyst. Fuel 332:126166. DOI:10.1016/j.fuel.2022.126166.

[14] Mathew, G. M., D. Raina, V. Narisetty, V. Kumar, S. Saran, A. Pugazhendi, R. Sindhu, A. Pandey, and P. Binod. 2021. Recent advances in biodiesel production: Challenges and solutions. Science of the Total Environment 794:148751. DOI:10.1016/j.scitotenv.2021.148751.

[15] Sun, X., S. Liu, S. Manickam, Y. Tao, J. Y. Yoon, and X. Xuan., 2023. Intensification of biodiesel production by hydrodynamic cavitation: A critical review. Renewable and Sustainable Energy Reviews 179:179. DOI:10.1016/j.rser.2023.113277

[16] Arslan E, Atelge MR, Kahraman N, Uenalan S., 2022. A study on the effects of nanoparticle addition to a diesel engine operating in dual fuel mode. Fuel 326:124847. ARTN 124847. https://doi.org/10.1016/j.fuel.2022.124847

[17] Yaashikaa PR, Kumar PS, Karishma S., 2022. Bio-derived catalysts for production of biodiesel: a review on feedstock, oil extraction methodologies, reactors and lifecycle assessment of biodiesel. Fuel 316:123379. ARTN 123379. https://doi.org/10.1016/j.fuel.2022.123379

[18] Osman AI, Lai ZY, Farghali M, Yiin CL, Elgarahy AM, Hammad A, Ihara I, Al-Fatesh AS, Rooney DW, Yap P-S., 2023. Optimizing biomass pathways to bioenergy and biochar application in electricity generation, biodiesel production, and biohydrogen production. Environ Chem Lett 21(5):2639–2705. https://doi.org/10.1007/s10311-023-01613-2

[19] Sarwer A, Hamed SM, Osman AI, Jamil F, Al-Muhtaseb AH, Alhajeri NS, Rooney DW, 2022. Algal biomass valorization for biofuel production and carbon sequestration: a review. Environ Chem Lett 20(5):2797–2851. https://doi.org/10.1007/s10311-022-01458-1

[20] Du C, Zhao X, Liu D, Lin CSK, Wilson K, Luque R, Clark J., 2016. Introduction: an overview of biofuels and production technologies. In: Handbook of biofuels production: processes and technologies, 2nd Ed. (98), pp 3–12. https://doi.org/10.1016/B978-0-08-100455-5.00001-1

[21] Ayadi M, Sarma SJ, Pachapur VL, Brar SK, Ben Cheikh R.,2016. History and Global Policy of Biofuels. Green Fuels Technol:Biofuels. https://doi.org/10.1007/978-3-319-30205-8_1

[22] Heidari S, Wood DA, 2021. Biodiesel production methods and feedstocks. Biodiesel Technol Appl. https://doi.org/10.1002/9781119724957.ch17

[23] Mayank Chhabra, Balraj Singh Saini & Gaurav Dwivedi, 2020. Optimization of the dual stage procedure of biodiesel synthesis from Neem oil using RSM based Box Behnken design. Energy Sources, Part A: Recovery, Utilization, and Environmental Effects. DOI:10.1080/15567036.2020.1771480

[24] Dwivedi, G., and M. P. Sharma. 2015. Application of Box–Behnken design in optimization of biodiesel yield from Pongamia oil and its stability analysis. Fuel 145:256–62. DOI:10.1016/j.fuel.2014.12.063.

[25] Onukwuli, D. O., L. N. Emembolu, C. N. Ude, S. O. Aliozo, and M. C. Menkiti, 2017. Optimization of biodiesel production from refined cotton seed oil and its characterization. Egyptian Journal of Petroleum 26 (1):103–10. DOI:10.1016/j.ejpe.2016.02.001.

[26] Xinyu, Z., G. Xu, Y. Yu, Y. Xiaobin, and Z. Bailiang. 2013. Optimization of transesterification of beef tallow for biodiesel production catalyzed by solid catalysts. Transactions of the Chinese Society of Agricultural Engineering 29:196–203.

[27] Karmakar A. et al.,2017. Process optimization of biodiesel production from Neem oil. Indian Journal of Agriculture Research 51 (6):529–35.

[28] Abdullah, A. T., J. Fieldhouse, and R. Brown, 2012. The optimisation of biodiesel production by using response surface methodology and its effect on diesel engine. 2nd International conference on environment science and biotechnology, Singapore. Vol 48. DOI: 10.7763/IPCBEE

[29] Aworanti, O. A., S. E. Agarry, and A. O. Ajani. 2013. Statistical optimization of process variables for biodiesel production from waste cooking oil using heterogeneous base catalyst. British Biotechnology Journal 3 (2):116–32. DOI:10.9734/BBJ/2013/1381.

[30] Omar, W. N. N. W., and N. A. S. Amin. 2011. Optimization of heterogeneous biodiesel production from waste cooking palm oil via response surface methodology. Biomass & Bioenergy 35:1329–38. DOI:10.1016/j.biombioe.2010.12.049.

[31] Ferreira, S. L. C., R. E. Bruns, H. S. Ferreira, G. D. Matos, J. M. David, G. C. Brand, E. G. P. da Silva, L. A. Portugal, P. S. Dos Reis, A. S. Souza, et al. 2007. Box-Behnken design: An alternative for the optimization of analytical methods. Analytica chimica acta 597:179–86. DOI:10.1016/j.aca.2007.07.011.

[32] Bezerraa, A., R. E. Santelli, E. P. Oliveiraa, L. S. Villar, and L. A. Escaleiraa. 2008. Response surface methodology (RSM) as a tool for optimization in analytical chemistry. Talanta 76:965–77. DOI:10.1016/j.talanta.2008.05.019

[33] Rezaei, R., M. Mohadesi, and G. R. Moradi. 2013. Optimization of biodiesel production using waste mussel shell catalyst. Fuel 109:534–41. DOI:10.1016/j.fuel.2013.03.004

[34] Charoenchaitrakoolm, M., and J. Thienmethangkoon. 2011. Statistical optimization for biodiesel production from waste frying oil through two-step catalyzed process. Fuel Processing Technology 92 (1):112–18. DOI:10.1016/j.fuproc.2010.09.012.

[35] O.M. Olatunji, I.T. Horsfall, E.V. Ubom, 2021. Response surface optimization approach to predict the maximum %biodiesel yield via transesterification of esterified shea butter oil by utilizing bio-catalysts, Current Research in Green and Sustainable Chemistry, Volume 4, 100167, ISSN 2666-0865, https://doi.org/10.1016/j.crgsc.2021.100167

[36] Masera, K., and A. K. Hossain. 2023. Advancement of biodiesel fuel quality and NOx emission control techniques. Renewable and Sustainable Energy Reviews 178:113235. DOI:10.1016/j.rser.2023.113235.

[37] Bora, P., L. J. Konwar, J. Boro, M. M. Phukan, D. Deka, and B. K. Konwar. 2014. Hybrid biofuels from non-edible oils: A comparative standpoint with corresponding biodiesel. Applied Energy 135:450–60. DOI:10.1016/j.apenergy.2014.08.114

[38] Saydut, A., S. Erdogan, A. B. Kafadar, C. Kaya, F. Aydin, and C. Hamamci. 2016. Process optimization for production of biodiesel from hazelnut oil, sunflower oil and their hybrid feedstock. Fuel 183:512–17. DOI:10.1016/j.fuel.2016.06.114.

[39] Gupta, J., M. Agarwal, and A. K. Dalai. 2016. Optimization of biodiesel production from mixture of edible and nonedible vegetable oils. Biocatalysis and Agricultural Biotechnology 8:112–20. DOI:10.1016/j.bcab.2016.08.014.

[40] Fadhil, A. B., A. W. Nayyef, and S. H. Sedeeq. 2020. Valorization of mixed radish seed oil and Prunus armeniaca L. oil as a promising feedstock for biodiesel production: Evaluation and analysis of biodiesels. Asia-Pacific Journal of Chemical Engineering 15 (1). DOI: 10.1002/apj.2390.

[41] Mujtaba, M. A., H. H. Masjuki, M. A. Kalam, H. C. Ong, M. Gul, M. Farooq, M. E. M. Soudagar, et al. 2020. Ultrasound-assisted process optimization and tribological characteristics of biodiesel from palm-sesame oil via response surface methodology and extreme learning machine - cuckoo search. Renewable Energy 158:202–14. DOI:10.1016/j.renene.2020.05.158

[42] Vargas, E. M., L. Ospina, M. C. Neves, L. A. C. Tarelho, and M. I. Nunes. 2021. Optimization of FAME production from blends of waste cooking oil and refined palm oil using biomass fly ash as a catalyst. Renewable Energy 163:1637–47. DOI:10.1016/j.renene.2020.10.030

[43] Vinayaka, A. S., B. Mahanty, E. R. Rene, and S. K. Behera. 2021. Biodiesel production by transesterification of a mixture of pongamia and neem oils. Biofuels 12 (2):187–95. DOI:10.1080/17597269.2018.1464874.

[44] Harisha, P., B. N. Anil Kumar, S. R. Tilak, and C. Ganesh. 2021. Production and optimization of biodiesel from composite Pongamia oil, animal fat oil and waste cooking oil using RSM. Materials Today: Proceedings 47 (xxxx):4901–05. DOI:10.1016/j.matpr.2021.06.322.

[45] Razzaq, L., M. M. Abbas, S. Miran, S. Asghar, S. Nawaz, M. E. M. Soudagar, N. Shaukat, I. Veza, S. Khalil, A. Abdelrahman, et al. 2022. Response surface methodology and artificial neural networks-based yield optimization of biodiesel sourced from mixture of palm and cotton seed oil. Sustainability 14 (10):6130. DOI:10.3390/su14106130.

[46] Kusumo, F., T. M. I. Mahlia, A. H. Shamsuddin, A. R. Ahmad, A. S. Silitonga, S. Dharma, M. Mofijur, F. Ideris, H. C. Ong, R. Sebayang, et al. 2022. Optimisation of biodiesel production from mixed Sterculia foetida and rice bran oil. International Journal of Ambient Energy 43 (1):4380–90. DOI:10.1080/01430750.2021.1888802.

[47] Srikanth, H. V., B. A. Praveena, G. L. Arunkumar, S. Balaji, N. Santhosh, K. Sridhar, and S. Bharath Kumar. 2023. Production optimisation of mixed oil (rubber seed oil–fish oil) feedstock using response surface methodology and artificial neural network. International Journal of Ambient Energy 44 (1):2336–46. DOI:10.1080/01430750.2023.2236107

[48] Brahma, S., B. Basumatary, S. F. Basumatary, B. Das, S. Brahma, S. L. Rokhum, and S. Basumatary. 2023. Biodiesel production from quinary oil mixture using highly efficient Musa chinensis based heterogeneous catalyst. Fuel 336:127150. DOI:10.1016/j.fuel.2022.127150.

[49] Van Eijck J, Batidzirai B, Faaij A., 2014. Current and future economic performance of first and second generation biofuels in developing countries. Appl Energy 135:115–141. https://doi.org/10.1016/j.apenergy.2014.08.015

[50] Kumar, S., M. K. Singhal, and M. P. Sharma. 2023. Improvement of oxidation stability and cold flow properties of biodiesel using mixed oil strategy. Waste and Biomass Valorization. DOI:10.1007/s12649-023-02170-z.

[51] Nouadjep S.N., Nso E., Gueguim Kana E.B., Kapseu C., 2019. Simplex lattice mixture design application for biodiesel production: Formulation and characterization of hybrid oil as feedstock, Fuel, Volume 252, Pages 135-142. https://doi.org/10.1016/j.fuel.2019.04.088

[52] Ghadge S.V., Raheman H., 2006. Process optimization for biodiesel production from mahua (Madhuca indica) oil using response surface methodology, Bioresource Technol. 97. 379–384.

[53] Derringer G., Suich R., 1980. Simultaneous optimization of several response variables. J. Qual Technol. 12:214-19.

[54] Lewis G.A., Mathieu D., Phan-Tann-Luu R., 1999. Pharmaceutical experimental design. New York, Marcel Dekker. 265-76.

[55] Botineștean Cristina, Hădărugă Nicoleta G., Hădărugă Daniel I., Jianu I., 2012. Fatty Acids Composition by Gas Chromatography –Mass Spectrometry (GC-MS) and most important physicalchemicals parameters of Tomato Seed Oil Journal of Agroalimentary Processes and Technologies.18(1) 89-94.

[56] Betiku E., Okunsolawo S.S., Ajala S.O., Odedele O. S., 2015. Performance evaluation of artificial neural network coupled with generic algorithm and response surface methodology in modeling and optimization of biodiesel production process parameters from shea tree (Vitellaria paradoxa) nut butter. Renewable Energy. 76: 408-417.

[57] Leung D.Y.C., Guo Y., 2006. Transesterification of neat and used frying oil: optimization for biodiesel production, Fuel Process. Technol. 87: 883–90.

[58] Yuan X., Liu J., Zeng G., Shi J., Tong J., Huang G., 2008. Optimization of conversion of waste rapeseed oil with high FFA to biodiesel using response surface methodology, Renew. Energ. 33 1678–84.

[59] Khuri A.I. & Cornell J.A., 1987. Response surfaces: design and analysis. New York: Marcel Dekker. 1987.

[60] Atapour, M., Kariminia, H. R., Moslehabadi, P. M., 2014. Optimization of biodiesel production by alkali-catalyzed transesterification of used frying oil. Process Saf Environ. 92(2), 179-185.

[61] Silva G. F., Camargo F. L., Ferreira A. L., 2011. Application of response surface methodology for optimization of biodiesel production by transesterification of soybean oil with ethanol. Fuel Process Technol. 92(3), 407-13.

[62] KoohiKamali S., Tan C. P., Ling T. C., 2012. Optimization of Sunflower Oil Transesterification Process Using Sodium Methoxide. The Scientific World Journal Volume 2012, Article ID 475027. DOI:10.1100/2012/475027

[63] Mirhosseini H., Tan C. P., Taherian A. R., Boo H. C., 2009. Modeling the physicochemical properties of orange beverage emulsion as function of main emulsion components using response surface methodology. Carbohydrate Polymers. 75 (3), pp. 512–520.

[64] Almaliki S., Himoud M., Jabar S., 2019. A Stepwise Regression Algorithm for Prognostication Draft Requirements of Disk Plough. Journal of Engineering and Applied Sciences 14 (special issue 8): 10335-40.

[65] Ghafoori S., Mehrvar M., Chan P. K., 2014. A statistical experimental design approach for photochemical degradation of aqueous polyacrylic acid using photo-Fenton-like process. Polymer Degradation and Stability. 110: 492-497.

[66] Mansourpoor M., Shariati A., 2012. Optimization of Biodiesel Production from Sunflower Oil Using Response Surface Methodology. J Chem Eng Process Technol. 3:141. DOI:10.4172/2157-7048.1000141.

[67] Jeong G.-T., Park D.-H., 2009. Optimization of Biodiesel Production from Castor Oil Using Response Surface Methodolog.y Appl. Biochem. Biotechnol. 156:431–441

[68] Dawodu F.A., Ayodele O.O, Bolanle-Ojo T., 2014. Biodiesel production from sesamum indicumL. Seed oil: an optimization study. Egyptian Journal of Petroleum; 23, 191-199.

[69] Kılıç M., Uzun B. B., Pütün E., Pütün Ayşe E.,2013. Optimization of biodiesel production from castor oil using factorial design. Fuel Processing Technology. 111: 105–110.

[70] Suherman, Suherman, Ilmi Abdullah, Muhammad Sabri, and Arridina Susan Silitonga. 2023. Evaluation of Physicochemical Properties Composite Biodiesel from Waste Cooking Oil and Schleichera oleosa Oil. Energies 16, no. 15: 5771. https://doi.org/10.3390/en16155771

[71] Hamze H., Akia M., Yazdani F., 2015. Optimization of biodiesel production from the waste cooking oil using response surface methodology. Process Saf Environ. 94, 1-10.

[72] Giwa Solomon, Adekomaya Oludaisi, Nwaokocha Collins, 2016. Potential hybrid feedstock for biodiesel production in the tropics. Front. Energy. DOI:10.1007/s11708-016-0408-8.

[73] Fasano E., Bono-Blay F., Cirillo T., Montuori P., Lacorte S., 2012. Migration of phthalates, alkylphenol, bisphenol A and di(2-ethylhexyl)adipate from food packaging. Food Control (27) 132−138.

[74] Rudel, R. A.; Dodson, R. E.; Perovich, L. J.; Morello-Frosch, R. et al., 2010. Semi-volatile endocrine-disrupting compounds in paried indoor and outdoor air in two northern California communities. Environ. Sci. Technol. 44, 6583−6590.

[75] Hoekman S. K., Broch A., Robbins C., Ceniceros E., Natarajan M., 2012. Review of biodiesel composition, properties, and specifications. Renewable and Sustainable Energy Reviews. 16: 143–169.

[76] Hung Y.S., Chen Y.H., Shang N.C., Chang C.H., Lu T.L., Chang C.Y., Shie J.L., 2010. Comparison of biodiesels produced from waste and virgin vegetable oils. Sustain. Environ. Res. 20(6), 417-422.